

STEPS TOWARD IMPROVED RADAR ESTIMATES OF CONVECTIVE RAINFALL USING
SPATIAL AVERAGES OBTAINED FROM RAIN GAUGE CLUSTERS*

J. Lane, T. Kasparis, and L. Jones
University of Central Florida
Orlando, Florida, USA

P. Glitto and D. Sharp
NOAA, National Weather Service
Melbourne, Florida, USA

F. Merceret
NASA, KSC Weather Office
KSC, Florida, USA

G. McFarquhar
National Center for Atmospheric Research
Boulder, Colorado, USA

B. Fisher
NASA, GSFC TRMM Office
Greenbelt, Maryland, USA

ABSTRACT

For the purpose of validating rainfall estimates from the Tropical Rainfall Measurement Mission's (TRMM) spaceborne precipitation radar, and from the National Weather Service's WSR-88D radar covering east central Florida, correlation with ground based rain gauge data is needed. However, a problem regularly encountered when correlating radar rainfall estimates with gauge measurements is the difference in measurement geometry. A gauge measures point rainfall, whereas radar estimates the average in a conical volume (the sample volume for WSR-88D rainfall estimation is $1^\circ \times 1$ km, with computed estimates available for each 5 min volume scan). Unfortunately, individual gauge positioning strategies for operational networks are often based on a combination of geopolitical factors, hydrologic reasoning, and the attempt to uniformly cover as much area as possible with a given number of gauges. Local examples include the St. Johns River Water Management District's network and the network at Kennedy Space Center (KSC) which have average site separations of 20 km and 5 km, respectively. Such spacing is generally sufficient for stratiform precipitation events since associated rainfall tends to be more spatially and temporally uniform. But for convective rains, the predominant form of precipitation in the tropics, the time rate of change of Z can be quite large. Moreover, precipitation cores of discrete convective cells could pass undetected between gauges while the occasional rapid movement of others could cause additional correlation errors. We propose to mitigate these difficulties by comparing spatially averaged rainfall rates derived from gauge measurements with corresponding spatially averaged radar estimates. Gauges are arranged in clusters of three with separations corresponding to convective cell dimensions, about 1 to 2 km. Using an root mean square error function of spatially and temporally averaged rainfall estimates, optimized model parameters can be found for any Z - R relationship. This method can be used both for research relating to Z - R relationships and to improve real-time radar rainfall estimates.

1.0 INTRODUCTION

In many applications of water resources management, such as in agriculture and forestry, it is desirable to accurately determine areal rainfall amounts with a high temporal and spatial resolution. A microscale network (separations on the order of 1 to 3 km) of rain gauges provides a reliable solution to detailed rainfall mapping for city size areas, farms, or park lands. However, dense rain gauge networks are not cost effective or practical for larger geographical areas such as counties, states, or regional areas due to the sheer number of gauges required. After all, one of the primary justifications for the development of the National Weather Service (NWS) network of NEXRAD radar was that it would provide improved rainfall information by filling in estimates over areas where large gaps in gauges exist.

There are two issues associated with weather radar rainfall estimation; scan strategy and calibration of the rainfall estimation algorithm. Since the primary aim of the NWS is public safety, the chosen radar scanning technique is optimized for surveillance and warning of severe weather conditions. The

* Presented at the First International Conference on Geospatial Information in Agriculture and Forestry, Lake Buena Vista, Florida, 1-3 June 1998.

resulting volume scan strategy, beam width, and range resolution are therefore not optimized for rainfall estimation. The issue of radar rainfall algorithm calibration is a more complex problem. In the early days of weather radar, it was believed that a simple Z - R relation (Z is radar reflectivity and R is rainfall rate) would suffice to accurately estimate rainfall amounts from radar measurements. Previously, most research focused on finding the “best” Z - R relation. However, it is now common knowledge that this approach is a gross over simplification of the problem (Atlas, 1997). Recent work in this area has split into three directions: (1) a comprehensive data analysis based on the complete volume scan and time series of radar images; (2) the assumption that only a statistical approach will yield useful results, based on long time averages and large areas of measurement; and (3) the application of other measurement techniques and instruments such as polarimetric radar (Zrnice, 1997) and ground based disdrometers (Schönhuber, 1997) to enhance present capabilities.

The primary motivation of the work presented in this paper was to develop a useful method of combining and interpolating rain gauge data for the purpose of real-time rainfall mapping. For any geographical area larger than a few hundred square kilometers, the network of NWS radar provides the best available solution for rainfall mapping. In this case, clusters of densely spaced rain gauges, as well as single isolated gauges in the radar service area (Krajewski, 1997), may be used to improve radar rainfall algorithm calibration and subsequent real-time rainfall estimation accuracy.

For global coverage (macro or synoptic scale), NASA’s Tropical Rainfall Measurement Mission (TRMM) satellite radar provides the best rainfall mapping solution. Calibration and verification of the satellite radar measurements are performed by specific Ground Validation (GV) sites consisting of rain gauge networks and NWS WSR-88D radar. A robust gauge interpolation algorithm is essential to the successful implementation of reliable ground truth for calibration of the NWS rainfall algorithm and subsequent calibration of the TRMM satellite radar.

2.0 MATHEMATICAL DEVELOPMENT

2.1 CONSERVATION EQUATION

The general differential equation for conservation of a field variable is:

$$\frac{\partial f(\mathbf{r}, t)}{\partial t} = \dot{f}(\mathbf{r}, t) - \mathbf{u}(\mathbf{r}, t) \cdot \nabla f(\mathbf{r}, t) \quad (1)$$

where $f(\mathbf{r}, t)$ may be a meteorological quantity such as radar reflectivity Z or rainfall rate R , at a point in space defined by the location vector \mathbf{r} and time t . $f(\mathbf{r}, t)$ is moving with an advection velocity $\mathbf{u}(\mathbf{r}, t)$ which is in general also a function of the location vector \mathbf{r} and time t .

In order to evaluate the total time derivative term, $\dot{f}(\mathbf{r}, t)$, it is often convenient to transform to a *Lagrangian* frame of reference that is traveling with the advection velocity $\mathbf{u}(\mathbf{r}, t)$. If at $t = 0$, the origin of the earth coordinate system, or *Eulerian* frame of reference, and Lagrangian system coincide, then the location vector \mathbf{r}' in the Lagrangian frame is related to \mathbf{r} in the Eulerian frame by $\mathbf{r}' = \mathbf{r}(t) - \mathbf{u} t$ in the case of constant advection velocity (space and time independent). Since by definition the advection velocity is zero in the Lagrangian frame, Equation (1) reduces to:

$$\frac{\partial f(\mathbf{r}', t)}{\partial t} = \dot{f}(\mathbf{r}', t) \quad (2)$$

According to Equation (2), determination of the total time derivative of a atmospheric quantity such as Z or R is most easily accomplished in an Lagrangian coordinate system.

A useful approximation, which will lead to a spatial and temporal interpolation method for radar and rain gauge data, is to assume that the total time derivative term in Equation (1) is small compared to the advective term:

$$\frac{\partial f(\mathbf{r}, t)}{\partial t} \approx -\mathbf{u}(\mathbf{r}, t) \cdot \nabla f(\mathbf{r}, t) \quad (3)$$

There are two cases to consider: (1) temporal interpolation of radar data, and (2) spatial interpolation of rain gauge data.

2.2 INTERPOLATION OF RADAR DATA

Radar data can be treated as discrete time samples of two-dimensional functions of reflectivity data, $Z_n(x, y)$ where n is the time frame index and x and y are projections of the spherical coordinate data from three-dimensional space onto a two-dimensional ground coordinate system. The radar *base product* data are discrete samples of a volume scan $Z_n(x, y, z)$, where $Z_n(x, y)$ is calculated from a vertical composite of reflectivity, such as the maximum Z value in the z direction: $Z_n(x, y) = \underset{(z)}{\text{Max}}\{Z_n(x, y, z)\}$ (Crosson,

1996). Given $f(\mathbf{r}, nT) = Z_n(x, y)$, where T is the frame interval time (radar volume scan period), a solution to Equation (3) is:

$$f(\mathbf{r}, t) = Z_n(\mathbf{r} - \mathbf{u} t) \quad (4)$$

Radar data, in its original form, is not a continuous function of x and y . If an arbitrary area is considered, consisting of $k = 1 \dots N$ radar samples $\{x_{kn}, y_{kn}, Z_{kn}\}$ where x_{kn} and y_{kn} are the Cartesian coordinates of the projection of the reflectivity value Z_{kn} onto the x - y ground plane, Shepard's interpolation formula (Shepard, 1968) can be combined with Equation (4) for each time frame n :

$$Z_n(x, y, t) = \frac{\sum_{k=1}^N Z_{kn} \left((x - x'_{kn})^2 + (y - y'_{kn})^2 \right)^{-q}}{\sum_{k=1}^N \left((x - x'_{kn})^2 + (y - y'_{kn})^2 \right)^{-q}}, \quad t_n \leq t < t_{n+1} \quad (5)$$

$$x'_{kn} = x_{kn} + (t - t_n) u \cos \theta, \quad t_n \leq t < t_{n+1} \quad (6a)$$

$$y'_{kn} = y_{kn} + (t - t_n) u \sin \theta, \quad t_n \leq t < t_{n+1} \quad (6b)$$

where θ is the angle of \mathbf{u} measured from the x -axis so that $\mathbf{u} = \{u, \theta\}$. Note that a typical value for q is 2 (Shepard, 1968). Practical conditions on the choice of number of radar samples N in Equation (5) is based on the requirement that the interpolated section should be well within the area enclosed by the $\{x_{kn}, y_{kn}\}$ coordinates.

In practice, Equation (5) must be *cross-faded* with consecutive radar frames $Z_n(x, y, t)$ and $Z_{n+1}(x, y, t)$ in order to prevent discontinuities in the interpolation, due to the total time derivative term, \dot{Z}_n , which was ignored in the preceding derivation:

$$Z(x, y, t) = (1 - w(t)) Z_n(x, y, t) + w(t) Z_{n+1}(x, y, t), \quad t_n \leq t < t_{n+1} \quad (7a)$$

$$w(t) \equiv \frac{t - t_n}{t_{n+1} - t_n}, \quad t_n \leq t < t_{n+1} \quad (7b)$$

The advection velocity can be estimated (Ciach, 1997) by performing a cross-correlation between consecutive frames of reflectivity $Z_n(x, y, t_{n+1})$ and $Z_{n+1}(x, y, t_{n+1})$, based on Equations (5) and (6):

$$\rho_n(\mathbf{u}) = \int_A (Z_n(x, y, t_{n+1}) - \eta_n) (Z_{n+1}(x, y, t_{n+1}) - \mu_{n+1}) dA \quad (8)$$

where η_n is the average value of $Z_n(x, y, t_n)$ and μ_{n+1} is the average value of $Z_{n+1}(x, y, t_{n+1})$ over a region of area A . The best estimate for advection velocity is that which maximizes $\rho_n(\mathbf{u})$.

2.3 INTERPOLATION OF RAIN GAUGE DATA

Rain gauge data can be treated as discrete spatial samples of a continuous time function of rainfall rate $R_j(t)$ where the i th gauge position is located at $\mathbf{r}_j = \{x_j, y_j\}$.

Given $f(\mathbf{r}_j, t) = R_j(t)$, a solution (Lane, 1997) to Equation (3) is:

$$f(\mathbf{r}, t) = R_j \left(t - \frac{(\mathbf{r} - \mathbf{r}_j) \cdot \mathbf{u}}{|\mathbf{u}|^2} \right) \quad (9)$$

Rain gauge data, in its original form, is not a continuous function of t . If a time sequence of rain rate data, consisting of $i = 1 \dots M$ samples $\{t_{ij}, R_{ij}\}$ where t_{ij} is the i th time at which the j th gauge acquires a rain rate sample of R_{ij} , Shepard's interpolation formula can be used with Equation (9) for each gauge location j :

$$R_j(x, y, t) = \frac{\sum_{i=1}^M R_{ij} |t - t'|^{-p}}{\sum_{i=1}^M |t - t'|^{-p}} \quad (10) \quad t' = t_{ij} + \frac{\cos \theta (x - x_j) + \sin \theta (y - y_j)}{u} \quad (11)$$

where a value of $p = 3$ seems to produce good results. The final interpolated rainfall rate is a superposition of the $R_j(x, y, t)$ from all L gauges of the network, again using Shepard's formula:

$$R(x, y, t) = \frac{\sum_{j=1}^L R_j(x, y, t) \left((x - x_j)^2 + (y - y_j)^2 \right)^{-q}}{\sum_{j=1}^L \left((x - x_j)^2 + (y - y_j)^2 \right)^{-q}} \quad (12)$$

A method of determining the advection velocity requires only a simple trigonometric computation. For example, note the cluster of three gauges shown in Figure 1. The advection time delay between gauges i and j can be formally found by performing a cross-correlation between the two gauges:

$$\rho(\tau_{ij}) = \int R_i(t - \tau_{ij}) R_j(t) dt \quad (13)$$

where the maximum of $\rho(\tau_{ij})$ gives the best estimate of the time delay τ_{ij} . Equation (13) is approximately equivalent to simply measuring the distance (in time) between correlated features of R_i and R_j , such as the rainfall rate peaks, as illustrated in Figure 2. The advection velocity can be estimated from the time delays determined from Equation (13), or by the graphical technique demonstrated in Figure 2:

$$\theta = \tan^{-1} \left\{ \frac{-\tau_{12}(x_3 - x_2) + \tau_{23}(x_2 - x_1)}{\tau_{12}(y_3 - y_2) + \tau_{23}(y_2 - y_1)} \right\} \quad (14a)$$

$$u = \frac{\cos \theta (x_2 - x_1) + \sin \theta (y_2 - y_1)}{\tau_{12}} = \frac{\cos \theta (x_3 - x_2) + \sin \theta (y_3 - y_2)}{\tau_{23}} \quad (14b)$$

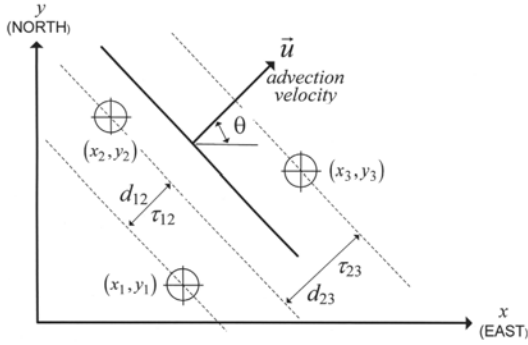


Figure 1. Determination of Advection Velocity from Adjacent Gauges Using Triangulation.

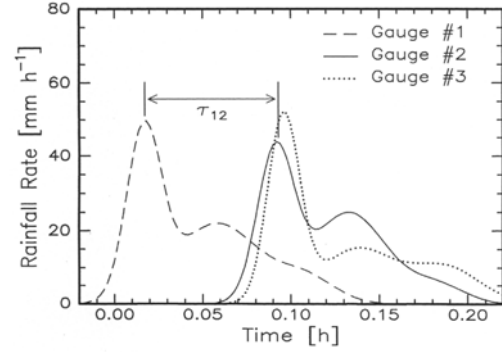


Figure 2. Three Adjacent Gauges Showing Delay Time Between Correlated Features of Rainfall Rate.

3.0 EXPERIMENTAL RESULTS

3.1 INTERPOLATION OF NWS RADAR AND TRMM RAIN GAUGE DATA

The data that will be used to demonstrate the concepts from the previous section was acquired on June 14, 1997, 18:00 through 18:40 UTC at KSC. Three TRMM/KSC rain gauges were used for this analysis, corresponding to site numbers 017, 018, and 020. The gauges are tipping buckets (manufactured by Qualimetric), physically located at the lightning detection sites as shown on the map of Figure 3. The circle surrounding the gauges in Figure 3 is the interpolation area that was used to process and compare the gauge and radar data. The corresponding radar is from the Melbourne WSR-88D (KMLB) station.

Using the rain gauge interpolation formula, Equation (12), $R(x_j, y_j, t)$ for the three TRMM/KSC gauges is plotted in Figures 4, where $j = 1, 2, 3$ corresponds to locations of gauges 017, 018, and 020. The rain rate in Figures 4 is equivalent to the raw tipping bucket data interpolated in time using a constant sample interval of 60 s. Also shown in Figures 4 is the interpolated NWS radar reflectivity, $Z(x_j, y_j, t)$, using Equations (7) and the lowest elevation scan data (base scan, 0.5° elevation), and again applying a sample interval of 60 s. Figures 5 show 120 s time intervals, again using Equations (7) and (12) to interpolate the rainfall and radar data over the circle surrounding the TRMM gauge locations. The rainfall rate map is converted to dBZ in Figures 5, using a power-law Z-R relation:

$$Z = a R^b \quad (15)$$

($a = 60$ and $b = 1.7$) so that the radar and gauge data can be easily compared. Note that black is equivalent to 45 dBZ, while white is equal to 30 dBZ, with shades of gray in between those values. This choice of gray level shading makes for easier comparison of the rain rate maps.

3.2 RMS GAUGE-RADAR ERROR

In order to determine an optimum set of Z-R coefficients a and b in Equation (15), a *root-mean-square* (RMS) error function can be defined, based on the differences between the j th rain gauge data and radar data (base scan or vertical reflectivity composite) above the j th gauge location:

$$E_j(a, b) = \left\{ \frac{1}{N} \sum_{n=1}^N \left[a R^b(x_j, y_j, t_n) - Z(x_j, y_j, t_n) \right]^2 \right\}^{1/2} \quad (16)$$

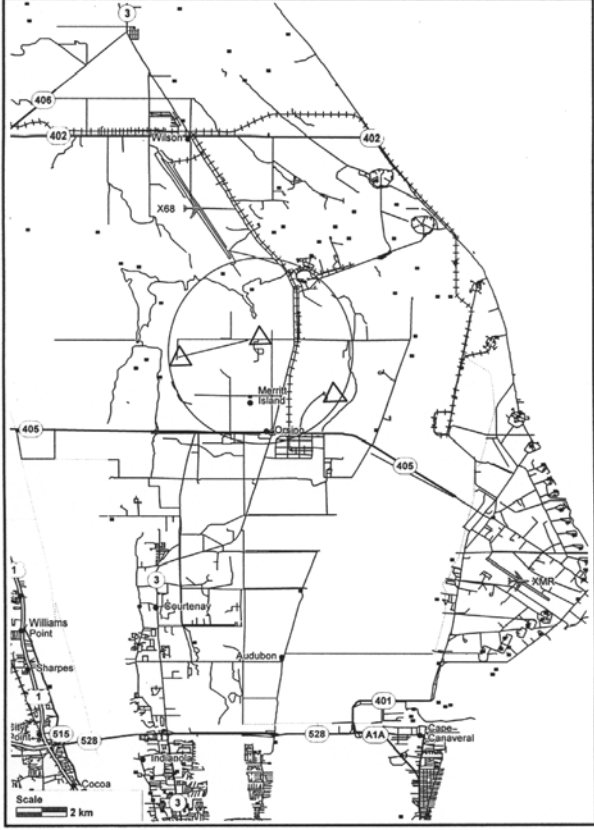


Figure 3. Map of TRMM/KSC Gauge Test Site.

where again the interpolation formulas from Equation (7) and (12) are used. Plots of $E_j(a, b)$ for $j = 1, 2$, and 3 are shown in Figures 6a, 6c, and 6e. Note that N is the number of 60 s time intervals in Figures 4. An RMS error function based on the arithmetic average of three gauge locations can also be defined as:

$$E_A(a, b) = \left\{ \frac{1}{N} \sum_{n=1}^N \left[\frac{1}{3} \sum_{j=1}^3 a R^b(x_j, y_j, t_n) - \frac{1}{3} \sum_{j=1}^3 Z(x_j, y_j, t_n) \right]^2 \right\}^{1/2} \quad (17)$$

A plot of $E_A(a, b)$ for the data of Figures 4, is shown in Figure 6g. Finally, an RMS error function can be defined, based on the area averaged interpolated rain gauge and interpolated radar reflectivity:

$$E(a, b) = \left\{ \frac{1}{N} \sum_{n=1}^N \left[\frac{1}{A} \int_A a R^b(x, y, t_n) dA - \frac{1}{A} \int_A Z(x, y, t_n) dA \right]^2 \right\}^{1/2} \quad (18)$$

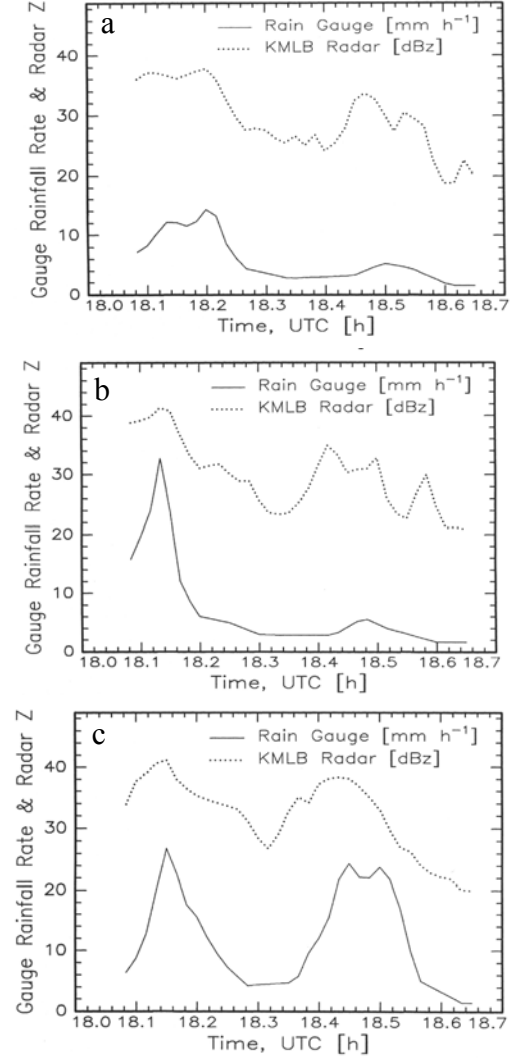
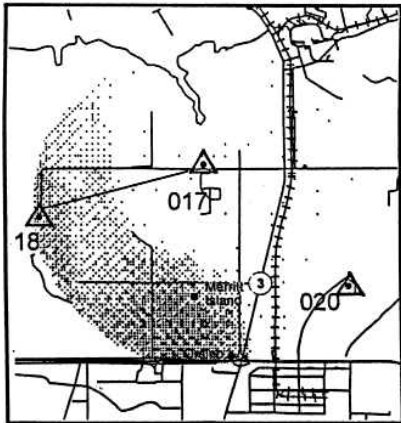
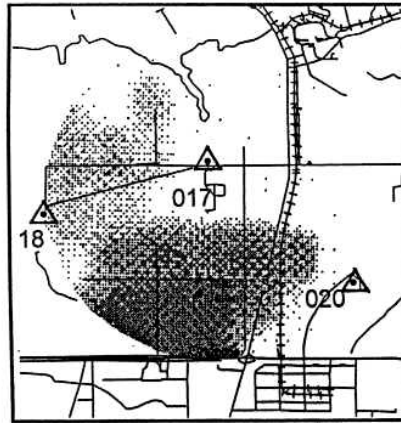


Figure 4. TRMM/KSC Rain Gauge and Melbourne NEXRAD Interpolated Data, June 14, 1997; (a) Gauge 017; (b) Gauge 018; and (c) Gauge 020.

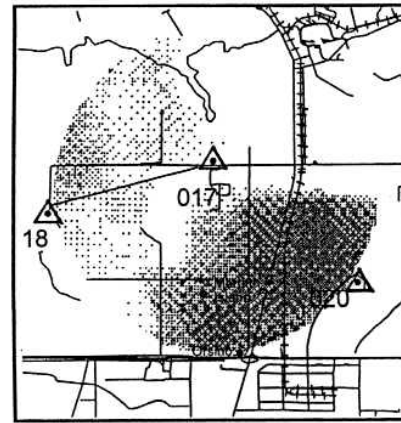
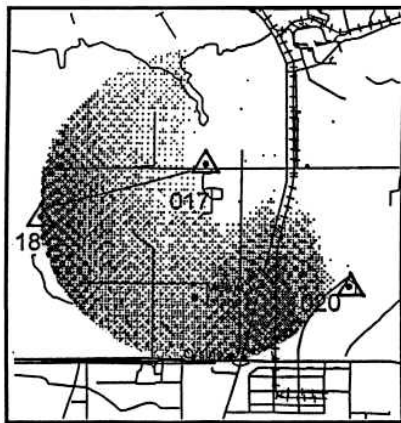
KSC/TRMM Rain Gauges



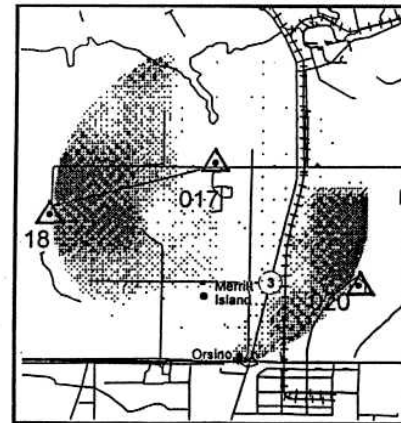
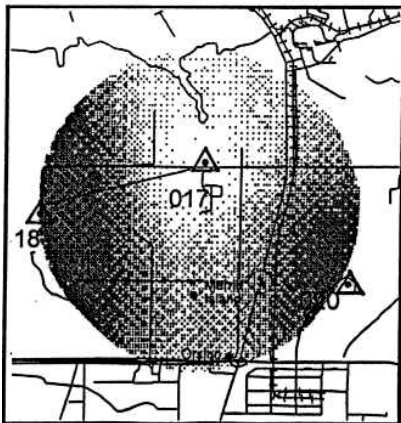
KMLB WSR-88D



$t = 18:05:00$ UTC



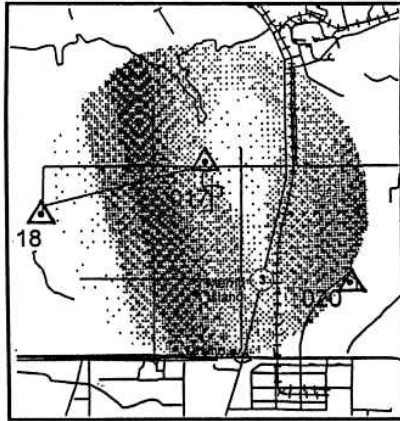
$t = 18:07:00$ UTC



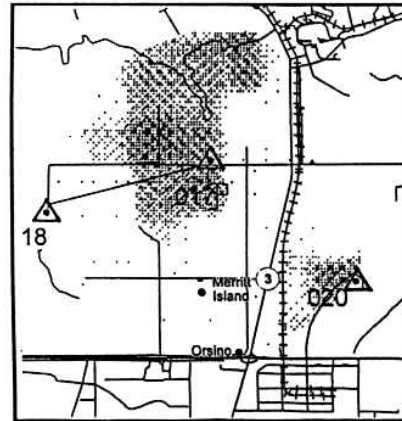
$t = 18:09:00$ UTC

Figure 5. Interpolated Rainfall Maps

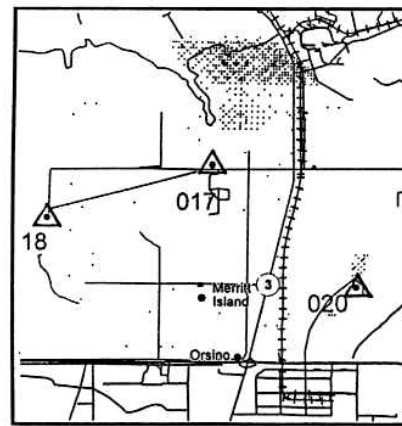
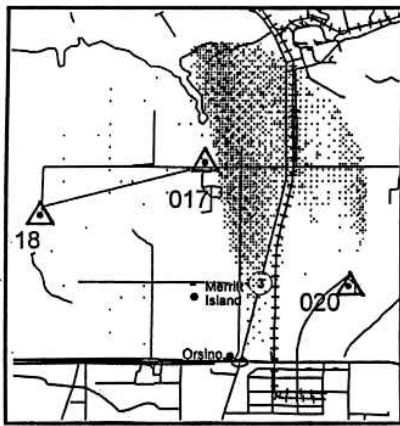
KSC/TRMM Rain Gauges



KMLB WSR-88D



$t = 18:11:00$ UTC



$t = 18:13:00$ UTC

Figure 5 (continued). Interpolated Rainfall, Based on TRMM/KSC and Melbourne NEXRAD Data, June 14, 1997.

A plot of $E(a,b)$ for the data of Figures 4, is shown in Figure 6h. The RMS error and linear regression plots of Figures 6, based on Equations (16) through (18), immediately reveal an error surface minimum, representing the optimal choice of the Z-R coefficients a and b in Equation (15). When the optimal Z-R coefficients from Figures 6a, 6c, and 6e are used to calculate radar rainfall rate from reflectivity data above the j th gauge, the best possible match, in a *least squares* sense, results as shown in Figures 7. Note that the RMS surface minimum agrees with the linear regression results of Figures 6b, 6d, and 6f, within quantization error of the RMS surface plots. (Also, note the time delay in Figure 7c between gauge and radar data, most likely due to advection and/or the fall time of drops above the gauge).

Another conclusion that can be inferred from the error surface plots of Figures 6, is the relative improvement of gauge rainfall to radar rainfall correlation. Figure 8a shows comparison of the minimum RMS error based on Equations (16) through (18) for the June 14, 1997 KSC data. It is clear from this graph that the spatial averaging method results in a choice of Z-R parameters which yield the minimum RMS error. Figures 8b and 8c show similar comparisons for two other rainfall events.

4.0 VALIDATING RADAR RAINFALL DATA

Rainfall is estimated by the Weather Service Radar 1988 Doppler (WSR-88D) by processing base reflectivity data taken from a 1 km x 1 km sample volume at approximately 3000 ft. (1 km). The data is processed through a series of algorithms and output is available each volume scan (5 min). From the output base reflectivity Z , rainfall rates R are computed using the system default equation, $Z = 300R^{1.4}$. Past radar rainfall studies conducted at the National Weather Service Office in Melbourne, Florida (NWSO MLB) used a network of more than 120 rain gauges to validate radar rainfall estimates. Rainfall

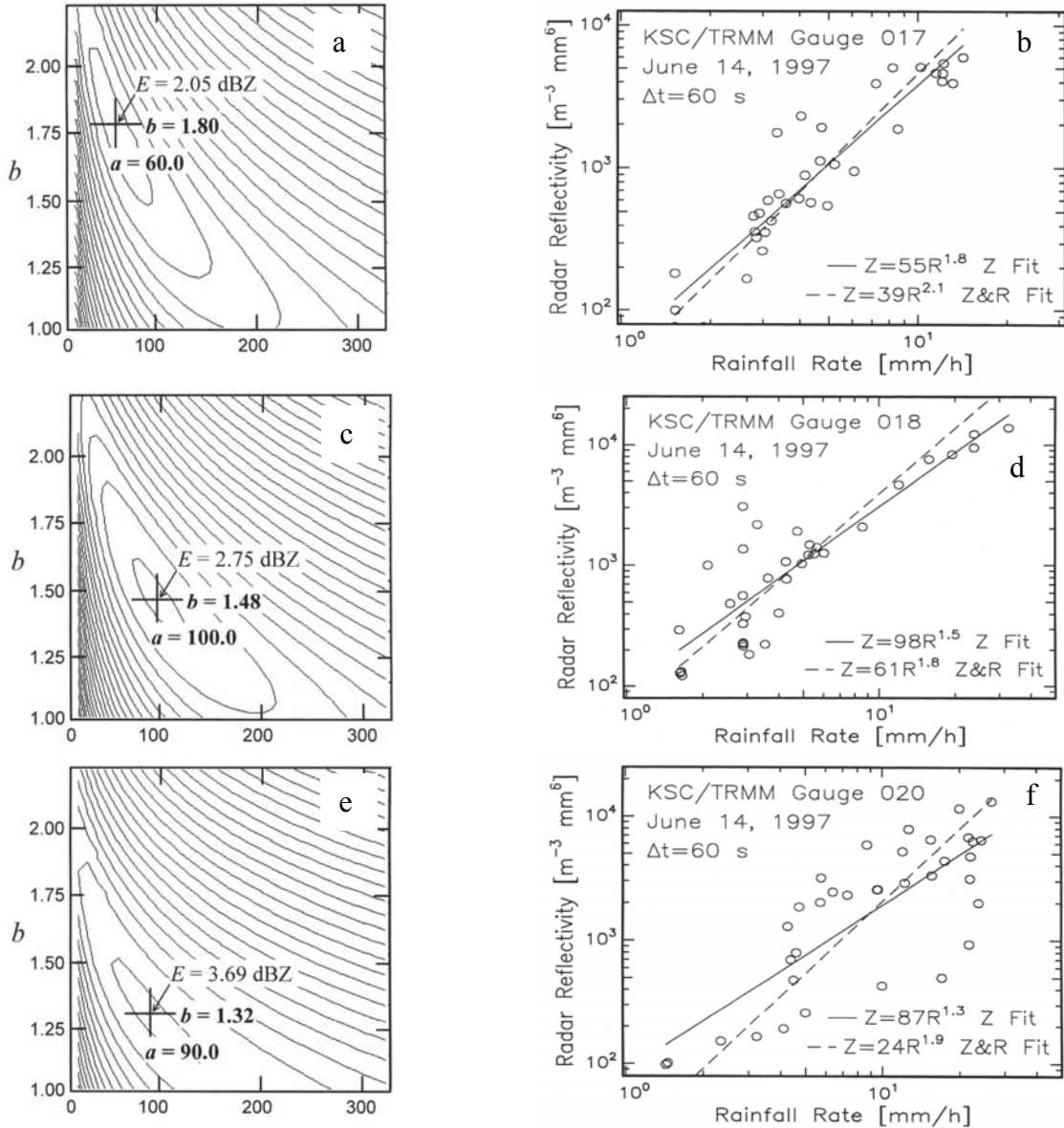


Figure 6. RMS and Linear Regression Plots Based on Data from Figures 4. (a) and (b) Gauge 017; (c) and (d) Gauge 018; (e) and (f) Gauge 020. Also Plotted (dashed lines) is Linear Regression with Equally Weighted R and Z (see Appendix).

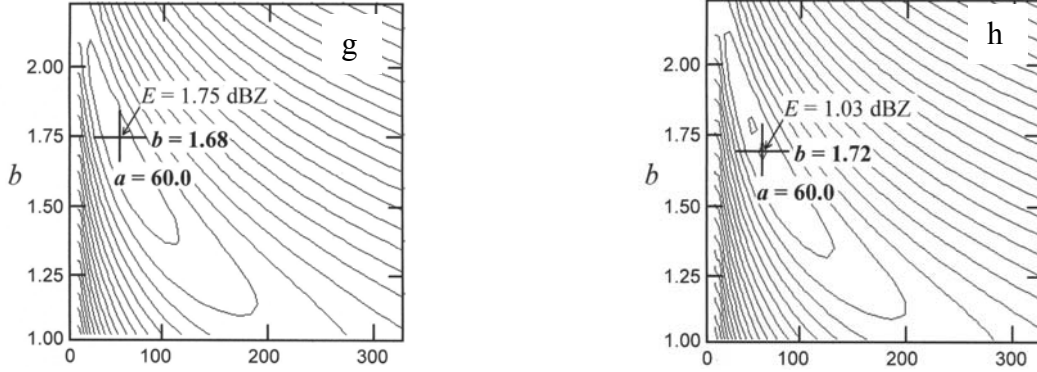


Figure 6 (continued). (g) RMS Error Based on Arithmetic Average of Gauges and Radar Data Using Equation (17) and (h) RMS Error Based on Spatial Integral of Gauges and Radar Data Using Equation (18).

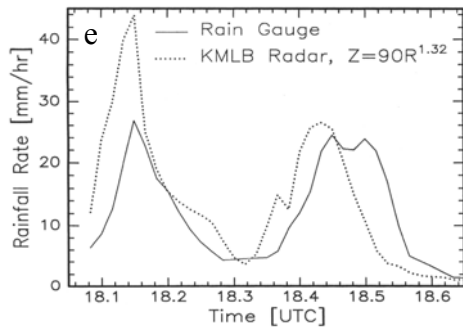
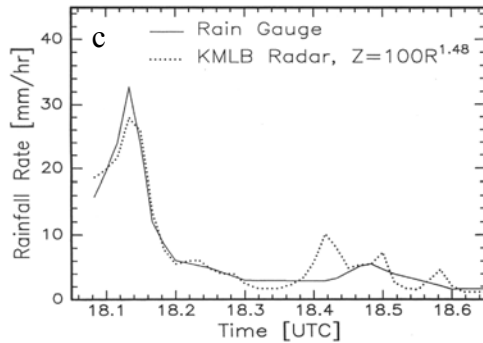
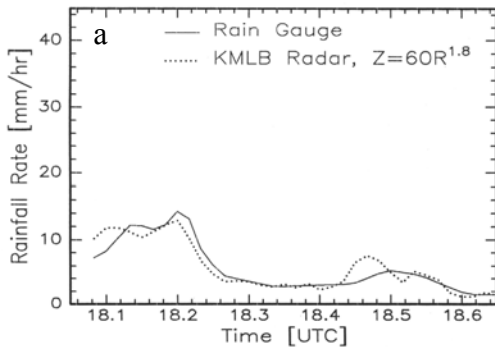


Figure 7. Radar Rainfall Based on Results from Figures 6a through 6f. (a) Site 017; (b) Site 018; (c) Site 020.

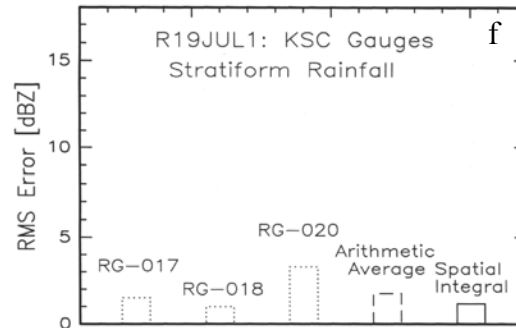
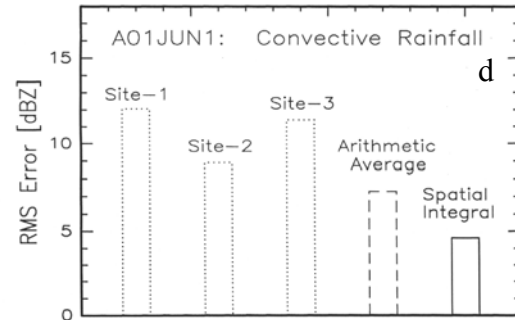
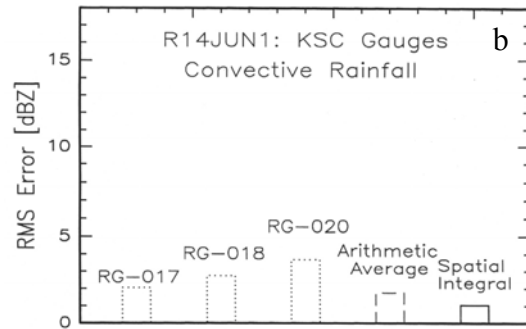


Figure 8. Comparisons of Z-R Determined from Equations (16), (17), and (18). (a) KSC - 14jun97; (b) Palm Bay, FL - 01jun97; (c) KSC - 19jul97.

data was archived during two tropical systems that affected east central Florida, Tropical Cyclone Gordon (1994) and Tropical Cyclone Jerry (1995). From the archived data, a file that contained a running total of estimated rainfall was compared with correspondent rain gauge locations.

There are many inherent problems with comparing a point measurement from a rain gauge with a radar estimate, taken instantaneously over a volume every 5 min. While the studies yielded results that were beneficial to NWS MLB operations (through algorithm adaptable parameter and *Z-R* relationship adjustments), there were still several limitations with rainfall validation procedures that needed to be improved upon. Since it was unlikely that the actual rain gauge location was always centered under a particular radar data bin, an array of nine radar data bins was centered over the rain gauge location. Comparisons were made using the center bin and the best fit of the nine bins (best bin). The best bin was the best match of the nine bins centered over the gauge location. For example, if the rain gauge total was between the maximum and minimum values of the nine bins, then the gauge value was used as the best bin. If the gauge value was lower (higher) than the minimum (maximum) of the nine bins, the minimum (maximum) was used as the best bin. Calculations of mean radar bias, variance, and average difference were performed in these studies.

4.1 SPATIAL AVERAGING APPROACH

The spatial averaging presented in this paper could decrease some of the problems noted in the studies conducted at NWSO MLB. By clustering the rain gauges close together and interpolating radar data between volume scans, the radar data may be considered a continuous function for any given x, y, t . Interpolating the radar data between radar scans to correspond with the gauge readings taken every 60 s has some advantages over a comparison based on a radar sample taken every 5 min. Since rainfall is advecting (or partially advecting) across a gauge, a single “snapshot” taken by the radar each 5 min could miss heavy rainfall between samples. Gauge clusters better accommodate convective rainfall where tighter gradients of reflectivity and dynamic changes in rainfall rate can be more reasonably estimated. Interpolating between scans serves to decrease the differences between the gauge and the radar. By clustering three gauges close together, difficulties with a single gauge comparison (such as the gauge location not corresponding to radar bin location or gauge malfunction) will be minimized.

The NWS is moving forward quickly in its effort to integrate into operations mosaicing of rainfall data, where data from several radar are composited. The rainfall mosaic will benefit greatly from improved radar rainfall estimates. In the rainfall mosaic, radar rainfall estimates will have overlap with adjacent radar in many areas. In the locations that overlap, the forecaster at the River Forecast Center (RFC) will use either an average of estimates between the radar that overlap, or the maximum value. Often the overlap will occur at ranges beyond 90 nm (167 km), where severe underestimation and a large variance in rainfall estimates was shown to exist during two tropical systems (Glitto, 1997). The error associated with a cell with heavy rain moving over a gauge between volume scans could be reduced by interpolating the radar data between volume scans. By interpolating the radar data between 5 min scans and comparing with the average of 3 gauge readings taken every 60 s, a better estimate may be obtained. Furthermore, by comparing one gauge with a radar bin, problems may arise with the gauge location not always corresponding with the bin location. Even if the gauge is compared with an array of radar bins, the “best” of the nine bins may be well above or below the gauge reading. In mosaicing radar estimated rainfall, using an average or maximum between overlapping radar sites may not work out well in many cases, since overlap is often at ranges beyond 90 nm, where a large variance in values and underestimation may exist. For instance, the maximum from three radar that are all severely underestimating rainfall is often still a poor estimate. By reducing the temporal scale and clustered spatial scale of the radar-gauge comparisons, better rainfall estimates may be obtained.

4.2 GAUGE SPACING

The question of optimum gauge spacing can be addressed by examining the correlation of adjacent gauges as defined by Equation (13). This is graphically shown by superimposing rainfall rate plots from adjacent gauges, such as that shown in Figure 2. As the separation of gauges is increased, the time delay of correlated features of the rainfall rates also increases. As the separation continues to increase, the rates become uncorrelated so that it is no longer possible to identify related features and is therefore not possible to extract a physically meaningful time delay. Another way of looking at the question of gauge spacing is to compare the total time derivative term of Equation (1) to the advective term. When the spacing is small, the advective term dominates and Equation (3) is an approximation of the rainfall at adjacent gauge sites. Physically, the concept of gauge correlation is simply that the gauges should be far enough apart to get a good “view” of a single convective cell as it passes over a gauge cluster site. When the distance is too large, adjacent gauge sites are no longer measuring the same convective cell. These qualitative specifications for spacing are very dependent on the extent of the convective cells within a storm system. The best strategy is to find a spacing small enough that satisfies these requirements for most storm systems, while maintaining the maximum separation possible. Based on the results presented in this work, a recommended spacing is 0.5 to 2 km. These distances are based on Florida summer thunderstorm characteristics, and may be different for other locations and time of year. This question will undoubtedly be a topic for future work.

5.0 SUMMARY

An algorithm for combining and interpolating rain gauge data for the purpose of real-time rainfall mapping, based on an advection transformation and Shepard’s formula, has been presented in this paper. Preliminary data provides evidence that this interpolation processing scheme can lead to improved charting of areal rainfall over microscale gauge networks, with immediate applications in forestry and agriculture. By integrating the spatially interpolated gauge and radar rainfall rates over microscale gauge clusters, the effects of advection and gravitational sorting of drops are reduced so that accurate areal average rainfalls may be generated with high temporal resolution. This method of gauge to radar comparison is suggestive of the *Window Probability Matching Method* (WPMM; Rosenfeld, 1994), but in this case both the gauge and radar are windowed in space. When spatially averaged gauge and radar rainfalls are compared in this way, other useful applications may be sought such as radar algorithm calibration, compositing of multiple weather radar, and calibration and verification of NASA’s TRMM satellite. These topics of investigation represent areas of future work.

6.0 REFERENCES

- D. Atlas, D. Rosenfeld, and A. R. Jameson, "Evolution of Radar Rainfall Measurements: Steps and Mis-Steps." In *Weather Radar Technology for Water Resources Management*, B. Braga, Jr. and O. Massambani, IRTCUD and IHP-UNESCO, San Paulo, Brazil, Chap. I, Sec. 1, 1997.
- G. J. Ciach, W. F. Krajewski, E. N. Anagnostou, M. L. Baeck, J. A. Smith, J. R. McCollum, and A. Kruger, "Radar Rainfall Estimation for Ground Validation Studies of the Tropical Rainfall Measurement Mission," *Journal of Applied Meteorology*, Vol. 36, No. 6, pp. 735-747, June 1997.
- W. L. Crosson, C. E. Duchon, R. Raghavan, and S. J. Goodman, "Assessment of Rainfall Estimates Using a Standard Z-R Relationship and the Probability Matching Method Applied to Composite Radar Data in Central Florida," *Journal of Applied Meteorology*, Vol. 35, No. 8, pp. 1203-1219, August 1996.
- P. Glitto and Lt. B. Choy., "A Comparison of WSR-88D Storm Total Precipitation Performance during Two Tropical Systems following Changes to the Multiplicative Bias and Upper Reflectivity Threshold," *Weather and Forecasting*, Vol. 12, No. 3, Part 1, pp. 459-471, September 1997.
- W. Krajewski, "Rainfall Estimation Using Weather Radar and Ground Stations." In *Weather Radar Technology for Water Resources Management*, B. Braga, Jr. and O. Massambani, IRTCUD and IHP-UNESCO, San Paulo, Brazil, Chap. I, Sec. 4, 1997.
- J. Lane, T. Kasparis, and G. McFarquhar, "Acoustic Rain Gauge Array Experiment: Phase I." In *ERIM 4th International Conference on Remote Sensing for Marine and Coastal Environments*, Orlando, FL, pp. II-311 - II-320, 17-19 March 1997.
- D. Rosenfeld and E. Amitai, "The Window Probability Matching Method for Rainfall Measurements with Radar," *Journal of Applied Meteorology*, Vol. 33, pp. 682-693, 1994.
- M. Schönhuber, H. E. Urban, J. P. V. Poiars Baptista, W. L. Randeu, and M. Riedler, "Weather Radar Versus 2D-Video-Distrometer Data." In *Weather Radar Technology for Water Resources Management*, B. Braga, Jr. and O. Massambani, IRTCUD and IHP-UNESCO, San Paulo, Brazil, Chap. I, Sec. 10, 1997.
- D. A. Shepard, "A Two-Dimensional Interpolation Function for Irregularly-Spaced Data." In *23th National Conference of the Association for Computing Machinery*, Brandon/Systems Press, Inc., Princeton, NJ, pp. 133-145, 1968.
- D. S. Zrnich and A. V. Ryzhkov, "Polarimetric Measurements of Rain." In *Weather Radar Technology for Water Resources Management*, B. Braga, Jr. and O. Massambani, IRTCUD and IHP-UNESCO, San Paulo, Brazil, Chap. I, Sec. 3, 1997.

7.0 APPENDIX - DETERMINING COEFFICIENTS OF THE Z-R POWER-LAW

Determining the coefficients a and b of the Z-R power-law $Z = aR^b$ can be performed by fitting the measured data points of $\log Z$ and $\log R$ to a straight line:

$$y = y_0 + m x \quad (\text{A-1})$$

where $y = \log Z$, $x = \log R$, $a = 10^{y_0}$, and $b = m$. This curve fitting procedure is often referred to as *linear regression* for historical reasons. For a set of N data points (x_i, y_i) , the following sums can be defined:

$$S \equiv \sum_{i=1}^N 1 = N \quad S_x \equiv \sum_{i=1}^N x_i \quad S_y \equiv \sum_{i=1}^N y_i \quad S_{xx} \equiv \sum_{i=1}^N x_i^2 \quad S_{yy} \equiv \sum_{i=1}^N y_i^2 \quad S_{xy} \equiv \sum_{i=1}^N x_i y_i \quad (\text{A-2})$$

Standard linear regression results in solutions for y_0 and m :

$$y_0 = \frac{S_{xx}S_y - S_xS_{xy}}{S_{xx} - S_x^2} \quad m = \frac{S_{xy} - S_xS_y}{S_{xx} - S_x^2} \quad (\text{A-3})$$

Equation (3) is the result of minimizing the χ^2 error defined as:

$$\chi^2(y_0, m) = \sum_{i=1}^N (y_i - y_0 - m x_i)^2 \quad (\text{A-4})$$

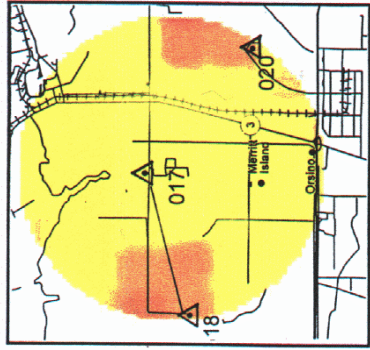
The preceding procedure minimizes the vertical distance between the data point y_i and the calculated point $y(x_i)$. The implication of this method is that all of the error in the data is contained in y_i . If the error is assumed to be equally distributed among both x_i and y_i , an alternate procedure is to minimize the perpendicular distance between (x_i, y_i) and the line $y = y_0 + m x$. In this case, the χ^2 error is defined as:

$$\chi^2(y_0, m) = \sum_{i=1}^N \frac{(y_i - y_0 - m x_i)^2}{1 + m^2} \quad (\text{A-5})$$

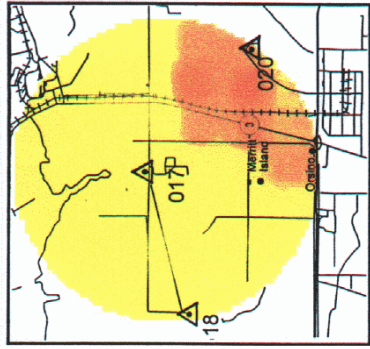
The new solutions for y_0 and m are now:

$$m = \frac{-\Gamma + \sqrt{\Lambda^2 + \Gamma^2}}{\Lambda} \quad y_0 = \frac{S_y - m S_x}{S} \quad (\text{A-6})$$

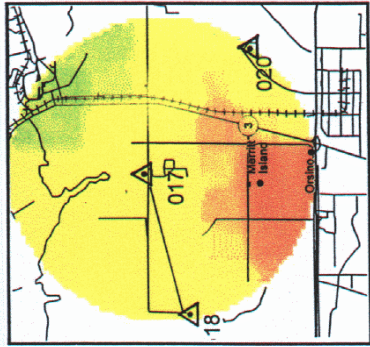
$$\Gamma \equiv S S_{xx} - S_x^2 - S S_{yy} - S_y^2 \quad \Lambda \equiv 2 (S S_{xy} - S_x S_y) \quad (\text{A-7})$$



$t = 18:05:00$ UTC



$t = 18:07:00$ UTC



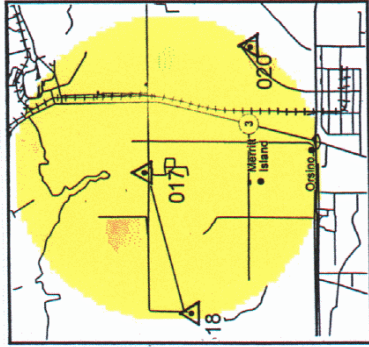
$t = 18:09:00$ UTC



$t = 18:11:00$ UTC

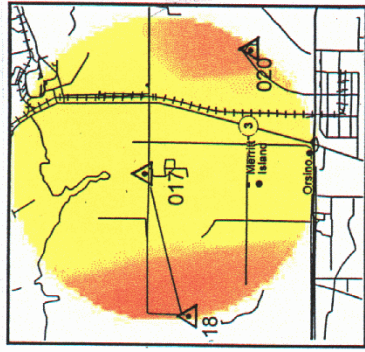


$t = 18:13:00$ UTC

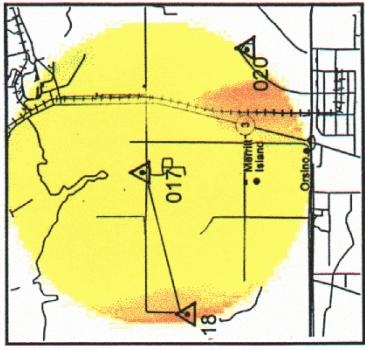


$t = 18:15:00$ UTC

Interpolated Melbourne NEXRAD Data over KSC Gauges, June 14, 1997.



$t = 18:05:00$ UTC



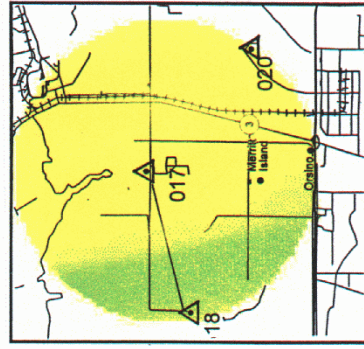
$t = 18:07:00$ UTC



$t = 18:11:00$ UTC



$t = 18:13:00$ UTC



$t = 18:15:00$ UTC

Interpolated Gauge Rainfall, Based on KSC Rain Gauge Data, June 14, 1997.